Analysis of Attenuation Poles using Closed-form Solutions for Bandpass Filters

Yoon mi Shin · Bom son Lee

Abstract

Very convenient equivalent circuits for the design of bandpass filters with an attenuation pole in the lower or upper stopband are provided together with necessary closed-form solutions. The proposed approach gives us much flexibility and simplifies the design of inserting attenuation poles.

Key words : Attenuation pole, Bandpass filter, Closed-form solution

Ⅰ. Introduction

The bandpass filters with attenuation poles using a capacitor connected in series with a short-circuited coaxial transmission line have been introduced in [1]~[3]. In the paper[4], the authors propose a modified Chebyshev bandpass filter design method by inserting attenuation poles into the upper or lower stopband using a lumped inductor or a capacitor in series with a resonator. However, several coupled equations must be solved simultaneously and iteratively in order to obtain all circuit values necessary for the filter design. In a new approach proposed in [5], it is suggested that in order to obtain the required filter response from the distorted response, the values of inverter elements on both sides of the resonator with an attenuation pole can be optimized using the linearity of the inverter element values of the conventional bandpass filter. This is an approximated approach. In this paper, we propose a quite clear and simple procedure of minimizing the distortion of transmission characteristics of the bandpass filter due to an attenuation pole in the lower or upper stopband, providing closed-form solutions. To show feasibility of the proposed method and correctness of the presented closed-form solutions, a design example is presented at the end of this paper.

Ⅱ. Analysis

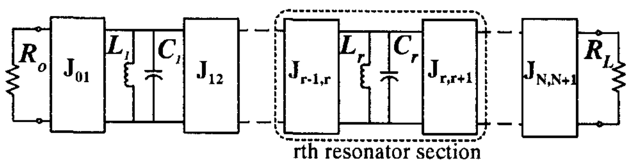

Fig. 1. Badpass filter network using admittance inverters.

The lowpass prototype filters can be transformed to the bandpass filters that use arbitrary parallel tuned resonators consisting of L_r' s and C_r' s (r=1, 2, ..., N), input resistance R_O and load resistance R_L, using admittance inverters as shown in Fig. 1[6],[7].

2-1 Resonator with Attenuation Pole in Lower Stopband

If an attenuation pole in the lower stopband is required, the rth resonator section in Fig. 1 needs to be replaced by the circuit as shown in Fig. 2(a). All the symbols used in Fig. 2 are relevant only in part 2-1 of section Ⅱ and 3-1 of section Ⅲ. The susceptance $Br_1(\omega)$ is given by

$$Br_1(\omega) = \frac{\omega C_p(1-\omega^2 L_r C_r)}{1-\omega^2 L_r(C_r+C_p)}. \tag{1}$$

The resonant frequency ω_0 and attenuation pole frequency ω_p of the circuit in Fig. 2(a) are $1/\sqrt{L_r C_r}$ (and 0) and $1/\sqrt{L_r(C_r+C_p)}$ (and ∞), respectively. The susceptance slope parameter br_1 of $Br_1(\omega)$ turns out to be that of the resonator consisting of only L_r and C_r shown in Fig. 1 and is given by

$$br_1 = \frac{\omega_o}{2}\left.\frac{dBr_1(\omega)}{d\omega}\right|_{\omega=\omega_O} = \sqrt{\frac{C_r}{L_r}} = \omega_o C_r. \tag{2}$$

The circuit in Fig. 2(b) is equivalent to that in Fig. 2(a) for any $k>0$, since the susceptance $Br_2(\omega)$ can be expressed as

$$Br_2(\omega) = \frac{k^2\omega C_p(1-\omega^2 L_r C_r)}{1-\omega^2 L_r(C_r+C_p)} = k^2 Br_1(\omega). \tag{3}$$

For the J-inverters on both sides of the resonant circuit, we can use a π network as shown in Fig. 2(c). For most of

Manuscript received September 9, 2001; revised October 24, 2001.
Department of Radio Engineering, Kyunghee University

practical filter designs, we need to absorb the negative capacitances of the adjacent inverters. In this case, we usually add positive capacitances in parallel with the resonator with an attenuation pole as shown in Fig. 2(c). Now, the susceptance $Br_3(\omega)$ in Fig. 2(c) can be expressed as

$$Br_3(\omega)=\frac{\omega C_p'(1-\omega^2L_r'C_r')}{1-\omega^2L_r'(C_r'+C_p')}+k\omega C, \quad (4)$$
$$C=C_{r-1,\ r}+C_{r,\ r+1}.$$

If we can find the perturbed values of L_r', C_r' and C_p' such that $Br_2(\omega)=Br_3(\omega)$, equivalence of the circuits in Fig. 2(b) and 2(c) are proved. By equating $Br_2(\omega)$ with $Br_3(\omega)$, we obtain the following closed-form solutions for L_r', C_r' and C_p' after somewhat lengthy algebraic manipulations.

$$L_r'=L_r\Bigg/\left[k^2-\frac{2kC}{C_p}+\left(\frac{C}{C_p}\right)^2\right] \quad (5)$$

$$C_r'=k^2C_r-\frac{(2C_r+C_p)kC}{C_p}+(C_r+C_p)\left(\frac{C}{C_p}\right)^2 \quad (6)$$

$$C_p'=k^2C_p-kC \quad (7)$$

We have many sets of solutions for L_r', C_r' and C_p' as k changes as a parameter. Actually, for any k unless any value of L_r', C_r' and C_p' turns out to be negative, the circuit in Fig. 2(c) is equivalent to that in Fig. 2(b), and thus to that in Fig. 2(a). The equivalent circuit in Fig. 2(c), together with the closed-form solutions given by (5)~(7), needs only to be substituted into the rth resonator section in Fig. 1 for realization of an attenuation pole in the lower stopband. Furthermore, we can choose a convenient k value without affecting the overall filter performance.

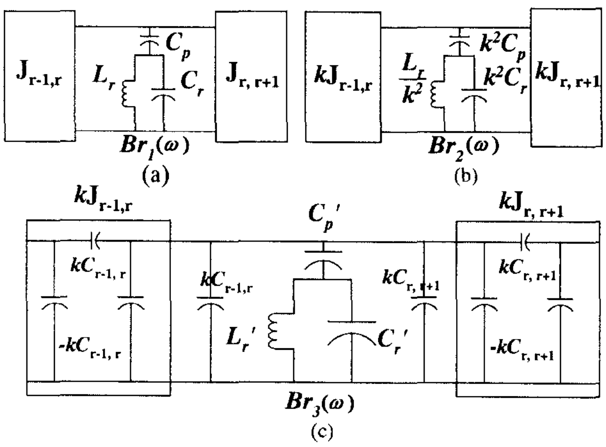

Fig. 2. Equivalent resonant circuits with an attenuation pole in the lower stopband (a) Basic circuit (b) Equivalent circuit (c) Equivalent circuit to absorb the negative capacitances.

2-2 Resonator with Attenuation Pole in Upper Stopband

If an attenuation pole in the upper stopband is required, the rth resonator section in Fig. 1 needs to be replaced by the circuit as shown in Fig. 3(a). All the symbols used in Fig. 3 are relevant only in part 2-2 of section Ⅱ and 3-2 of section Ⅲ. The susceptance $Br_1(\omega)$ is given by

$$Br_1(\omega)=\frac{1-\omega^2L_rC_r}{\omega[\omega^2L_rL_pC_r-(L_r+L_p)]}. \quad (8)$$

The resonant frequency ω_0 and attenuation pole frequency ω_p of the circuit in Fig. 3(a) are $1/\sqrt{L_rC_r}$ (and 0) and $\sqrt{(L_r+L_p)/L_rL_pC_r}$ (and ∞), respectively. The susceptance slope parameter br_1 of $Br_1(\omega)$ turns out to be that of the resonator consisting of only L_r and C_r shown in Fig. 1 and is given by

$$br_1=\frac{\omega_o}{2}\frac{dBr_1(\omega)}{d\omega}\bigg|_{\omega=\omega_o}=\sqrt{\frac{C_r}{L_r}}=\omega_oC_r. \quad (9)$$

The circuit in Fig. 3(b) is equivalent to that in Fig. 3(a) for any $k>0$, since the susceptance $Br_2(\omega)$ can be expressed as

$$Br_2(\omega)=\frac{k^2(1-\omega^2L_rC_r)}{\omega[\omega^2L_rL_pC_r-(L_r+L_p)]}=k^2Br_1(\omega). \quad (10)$$

For the J-inverters on both sides of the resonant circuit, we can use a π network as shown in Fig. 3(c). For most of practical filter designs, we need to absorb the negative capacitances of the adjacent inverters. In this case, we usually add positive capacitances in parallel with the resonator with an attenuation pole as shown in Fig. 3(c). Now, the susceptance $Br_3(\omega)$ in Fig. 3(c) is given by

$$Br_3(\omega)=\frac{1-\omega^2L_r'C_r'}{\omega[\omega^2L_r'L_p'C_r'-(L_r'+L_p')]}+k\omega C, \quad (11)$$
$$C=C_{r-1,\ r}+C_{r,\ r+1}$$

and the susceptance slope parameter br_3 is given by

$$br_3=\frac{\omega_o}{2}\frac{dBr_3(\omega)}{d\omega}\bigg|_{\omega=\omega_o}. \quad (12)$$

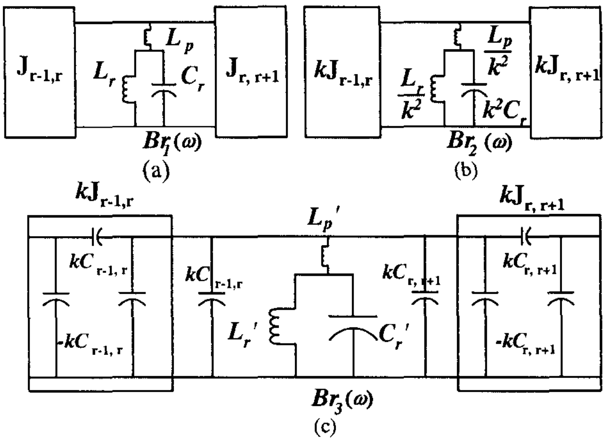

Fig. 3. Equivalent resonant circuits with an attenuation pole in the upper stopband (a) Basic circuit (b) Equivalent circuit (c) Equivalent circuit to absorb the negative capacitances.

For the equivalence of the circuits in Fig. 3(b) and 3(c) under narrowband conditions, we require that $Br_3(\omega_o) \rightarrow 0, Br_3(\omega_p) \rightarrow \infty$, and $br_3 = k^2 br_1 = k^2 \omega_o C_r$. After somewhat lengthy algebraic manipulations, we obtain the closed-form solutions for L_p', L_r', and C_r' given by

$$L_p' = \frac{1}{k^2 C_r(\omega_p^2 - \omega_o^2) + kC(2\omega_o^2 - \omega_p^2)} \tag{13}$$

$$L_r' = L_r \left[\frac{\omega_p^2}{k^2(\omega_p^2 - \omega_o^2) + kC\omega_o^4 L_r} - \frac{\omega_o^2}{k^2(\omega_p^2 - \omega_o^2) + kC\omega_o^2(2\omega_o^2 - \omega_o^2)L_r} \right] \tag{14}$$

$$C_r' = \frac{L_r' + L_p'}{\omega_p^2 L_r' L_p'}. \tag{15}$$

We have many sets of solutions for L_p', L_r', and C_r' as k changes as a parameter. Actually, for any k unless any value of L_p', L_r', and C_r' turns out to be negative, the circuit in Fig. 3(c) is practically equivalent to that in Fig. 3(b), and thus to that in Fig. 3(a). The equivalent circuit in Fig. 3(c), together with the closed-form solutions given by (13)~(15), needs only to be substituted into the rth resonator section in Fig. 1 for realization of an attenuation pole in the upper stopband. Furthermore, we can choose a convenient k value without affecting the overall filter performance.

Ⅲ. Design Examples

3-1 Design of Bandpass Filter with an Attenuation Pole in the Lower Stopband

Table 1. Specifications for a design example (attenuation pole in lower stopband).

Description	Specifications
Passband	2,110~2,170 MHz (Rx)
Passband ripple	0.1 dB
Attenuation pole frequency	1,980 MHz
Number of resonators (N)	3

Table 2. Values of filter element without attenuation pole (attenuation pole in lower stopband).

J_{01}, J_{34}	0.0066 mho	Lr(r=1, 2, 3)	0.9416 nH
J_{12}, J_{23}	0.0021 mho	Cr(r=1, 2, 3)	5.8751 pF

To show feasibility of the proposed method, we design a Chebyshev bandpass filter of which specifications are given in Table 1. To see the degree of distortion of the bandpass filter having an attenuation pole in the lower stopband, we plotted insertion losses (S_{21}' S) for four cases in Fig. 4 based on simulations using Ansoft Serenade V8.5. Case 1 is the one without an attenuation pole. The element values for Case 1 are summarized in Table 2. Case 2, Case 3 and Case 4 are according to Fig. 2(c) with (k=0.5, L_2'=25.2772nH, C_2'=0.1604pF, C_p'=0.0952pF), (k=1, L_2'=1.9607nH, C_2'=2.6117pF, C_p'=0.6837pF), and (k=10, L_2' =0.0100nH, C_2' =549.0534pF, C_p'=95.6235pF), respectively. The S_{21}'s for the cases from 2 to 4 are shown to be exactly the same, having a resonant frequency at 2,140 MHz and an attenuation pole frequency at 1,980 MHz. Off the resonant frequency of 2,140 MHz, they deviate somewhat from the insertion loss for Case 1 due to the effect of the inserted attenuation pole in the lower stopband.

3-2 Design of Bandpass Filter with an Attenuation Pole in the Upper Stopband

To show feasibility of the proposed method, we design a Chebyshev bandpass filter of which specifications are given in Table 3. In Fig. 5, we plotted insertion losses (S_{21}'S) for four cases.

Table 3. Specifications for a design example (attenuation pole in upper stopband).

Description	Specifications
Passband	1,920~1,980 MHz (Tx)
Passband ripple	0.1 dB
Attenuation pole frequency	2,110 MHz
Number of resonators (N)	3

Table 4. Values of filter element without attenuation pole (attenuation pole in upper stopband)

J_{01}, J_{34}	0.0072 mho	L_r (r=1, 2, 3)	0.9416 nH
J_{12}, J_{23}	0.0025 mho	C_r (r=1, 2, 3)	7.0760 pF

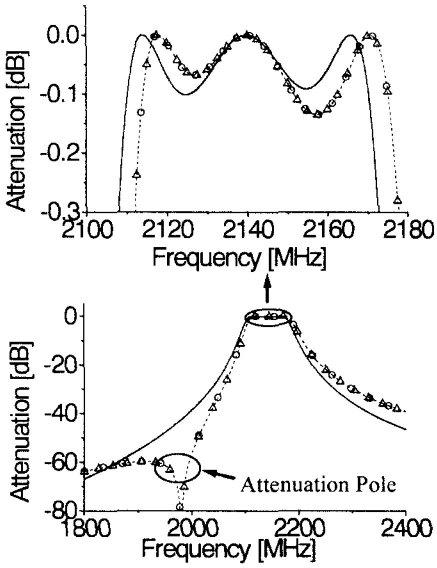

Fig. 4. Insertion losses (S_{21}'S) for case 1 to 4.

——— Case 1: without attenuation pole
------ Case 2: with attenuation pole (k=0.5)
○ Case 3: with attenuation pole (k=1)
△ Case 4: with attenuation pole (k=10)

Case 5 is the one without an attenuation pole. The element values for Case 5 are summarized in Table 4. Case 6, Case 7 and Case 8 are according to Fig. 3(c) with (k=0.5, $L_2{}'$ = 1.2989 nH, $C_2{}'$ = 4.7804 pF, $L_p{}'$ = 14.2190 nH), (k=1, $L_2{}'$ = 0.5240 nH, $C_2{}'$ = 12.1745 pF, $L_p{}'$ = 4.3194 nH), and (k=10, L'_2 = 0.0088 nH, $C_2{}'$ = 751.1656 pF, $L_p{}'$ = 0.0536 pH), respectively. The S_{21}'s for the cases from 6 to 8 are shown to be exactly the same, having a resonant frequency at 1,950 MHz and an attenuation pole frequency at 2,110 MHz. Off the resonant frequency of 1,950 MHz, they deviate somewhat from the insertion loss for Case 1 due to the effect of the inserted attenuation pole in the upper stopband.

3-3 Design of Duplexer

Fig. 6 shows the equivalent circuit of a duplexer with an attenuation pole in the lower and upper stopband. We design a duplexer using Table 1 and Table 3. In Fig. 6, the subscript U

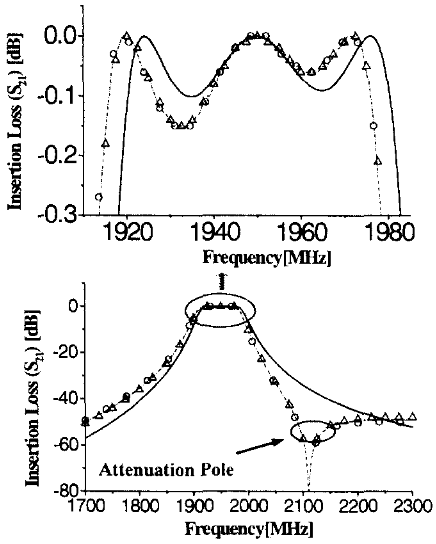

Fig. 5. Insertion losses (S_{21}'S) for case 5 to 8.

——— Case 5: without attenuation pole
------ Case 6: with attenuation pole (k=0.5)
○ Case7: with attenuation pole (k=1)
△ Case 8: with attenuation pole (k=10)

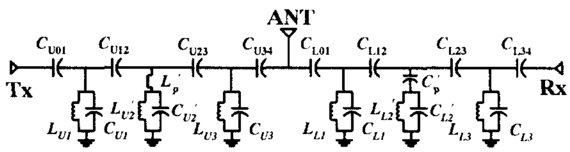

Fig. 6. Equivalent circuit of duplexer.

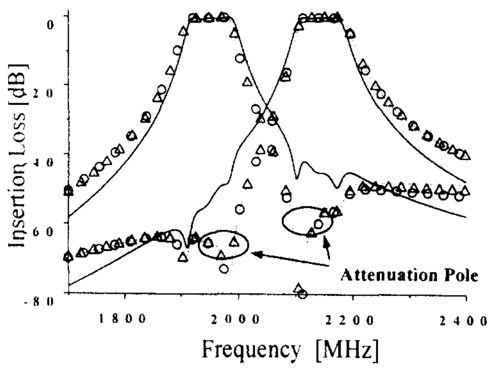

Fig. 7. Insertion losses (S_{21}'S) for case 9 to 12.

——— Case 9: without attenuation pole
------ Case 10: with attenuation pole (k=0.5)
○ Case 11: with attenuation pole (k=1)
△ Case 12: with attenuation pole (k=10)

and L denote upper and lower stopbands.

In Fig. 7, we plotted insertion losses for Case 9 through 12. Case 9 is the one without attenuation poles. The element values for Case 9 are summarized in Table 2 and Table 4. (Case 10, 11, 12) are the ones combining (Case 2, 3, 4) in design example A and (Case 6, 7, 8) in design example B, respectively. The insertion losses for the Cases from 10 to 11 are shown to be exactly the same, having a Tx resonant frequency at 1950MHz and Rx resonant frequency at 2,140 MHz and a Tx attenuation pole frequency at 2,110 MHz and a Rx attenuation pole frequency at 1980MHz. Off the Tx resonant frequency of 1,950 MHz andRx resonant frequency of 2,140 MHz, they deviate somewhat from the insertion loss for Case 1 due to the effect of the inserted attenuation pole in the lower and upper stopbands.

Ⅳ. Conclusion

Very convenient equivalent circuits together with closed-form solutions are provided as a solution to the problem of perturbed resonant circuits with an attenuation pole in the lower or upper stopband. The presented design examples for a Chebyshev bandpass filter verified the correctness of the solutions and showed the usefulness of the approach.

References

[1] H. Matsumoto, T. Yorita, Y. Ishikawa, and T. Nishikawa, "Miniaturized duplexer using rectangular coaxial dielectric resonators for cellular portable telephone", *IEICE Trans.*, vol. E74, no. 5, pp. 1214-1220, May 1991.

[2] T. Nishikawa, "RF front-end circuit components miniaturized using dielectric resonators for cellular portable telephones", *IEICE Trans.*, vol. E74, no. 6, pp. 1556-1562, June 1991.

[3] H. Matsumoto, and T. Nishikawa, "Design of miniaturized dielectric duplexer with attenuation poles", *IEICE Trans.*, vol. J76-C-1, no. 5, pp. 164-172 (Japanese), May 1993.

[4] J. S. Lim, and D. C. Park, " A modified chebyshev bandpass filter with attenuation poles in the stopband", *IEEE Trans. Microwave Theory & Tech.*, vol. 45, no. 6, pp. 898-904, June 1997.

[5] Y. J. Ko, J. H. Kim, and B. K. Kim, " A novel approach for the design of a bandpass filter with attenuation poles using a linear relationship", *IEICE Trans. ELECTRON*, vol. E82-C, no.7, pp. 1110-1115, July 1999.

[6] R. E. Collin, *Foundations for microwave engineering*, Second Edition, McGraw-Hill, Inc., 1992.

[7] G. L. Matthaei, L. Young, and E. M. T. Jones, *Microwave Filters, Impedance-Matching Networks and Coupling Structures*, New York: McGraw-Hill, 1964.

Yoon Mi Shin

received the B.S. degree in dept. of radio engineering from Kyunghee University in 1999 and is currently working on her the M.S. degree at the Kyunghee University. Her research interests are in the area of PBG, antenna and filter.

Bom Son Lee

received the B.S. degree in electric engineering from Seoul National University in 1982, and the M.S. degree in electronic engineering from State of Lincoln-Nebraska University in 1991, and the Ph. D. degree in electronic engineering in 1995. Since september 1995, he is professor in the school of Electronics & Information Engineering at Kyunghee Univ. His research interests are in the area of Antenna theory and Design and Wave propagation.